

Angular momentum dependence of the nuclear level density in the $A \approx 170$ – 200 region

M. Gohil, Pratap Roy,* K. Banerjee, C. Bhattacharya, S. Kundu, T. K. Rana, T. K. Ghosh, G. Mukherjee, R. Pandey, H. Pai, V. Srivastava, J. K. Meena, S. R. Banerjee, S. Mukhopadhyay, D. Pandit, S. Pal, and S. Bhattacharya
Variable Energy Cyclotron Centre, 1/AF, Bidhan Nagar, Kolkata 700064, India

(Received 16 September 2014; revised manuscript received 5 December 2014; published 14 January 2015)

Neutron evaporation spectra along with γ multiplicity has been measured from $^{201}\text{Tl}^*$, $^{185}\text{Re}^*$, and $^{169}\text{Tm}^*$ compound nuclei at the excitation energies of ~ 27 and 37 MeV. Statistical model analysis of the experimental data has been carried out to extract the value of the inverse level density parameter k at different angular-momentum (J) regions corresponding to different γ multiplicities. It is observed that, for the present systems the value of k remains almost constant for different J . The present results for the angular-momentum dependence of the nuclear level density (NLD) parameter \tilde{a} ($=A/k$), for nuclei with $A \sim 180$ are quite different from those obtained in earlier measurements in the case of light- and medium-mass systems. The present study provides useful information to understand the angular-momentum dependence of the NLD at different nuclear mass regions.

DOI: [10.1103/PhysRevC.91.014609](https://doi.org/10.1103/PhysRevC.91.014609)

PACS number(s): 25.70.Jj, 25.70.Gh, 24.10.Pa

I. INTRODUCTION

An accurate determination of nuclear level density (NLD) and information on its dependence on key nuclear parameters such as excitation energy and angular momentum (spin) is essential for precise estimation of nuclear reaction rates using statistical models. Although several theoretical as well as experimental attempts have been made in the past to understand the excitation-energy dependence of NLD; the information on its angular-momentum dependence is quite limited. Information on the angular-momentum dependence of nuclear level density can be obtained experimentally by measuring light-particle evaporation spectra in coincidence with the low-energy γ -ray multiplicity, which is directly related to the angular momentum populated in the nucleus. With the development of advanced γ -ray multiplicity detector arrays, it has been possible to carry out such measurements in recent times [1–6]. On the theoretical side, where the information on the variation of NLD over a wide range of excitation energy (E^*) and angular momentum (J) comes only from the phenomenology based semi-empirical formulations, the spin dependence in NLD is accounted for by two different approaches. In the first approach, applicable mostly at moderate E^* and J , the angular-momentum dependence is incorporated through the spin-dependent rotational energy [7],

$$E_{\text{rot}} = \frac{\hbar^2}{2\mathfrak{S}_{\text{eff}}} J(J+1), \quad (1)$$

with

$$\mathfrak{S}_{\text{eff}} = \mathfrak{S}_0(1 + \delta_1 J^2 + \delta_2 J^4). \quad (2)$$

Here $\mathfrak{S}_{\text{eff}}$ and \mathfrak{S}_0 are the effective and rigid-body moment of inertia of the system and δ_1 and δ_2 , known as the deformability coefficients, are adjustable parameters that provide a range of choices for the spin dependence of the level density [8]. The rotational energy is subtracted from the excitation energy and

the effective energy is used to calculate the NLD by using the standard level density formula [9]. In the second approach, mostly applicable for low E^* and J , the spin dependence is introduced in the total level density by a multiplicative Gaussian function [$\exp[-(J + \frac{1}{2})^2/(2\sigma^2)]$] [10], where the width of the Gaussian is determined by the temperature-dependent (T -dependent) spin cutoff factor $\sigma = [(\mathfrak{S}_0 T)/\hbar^2]^{1/2}$. At high excitation energy (i.e., for $E^* \gg E_{\text{rot}}$) these two approaches become equivalent. In both the approaches the spin dependence in NLD has been incorporated independently and there is no additional dependence of the level density parameter on angular momentum or deformation. These prescriptions have been tested mostly with the inclusive particle spectra and found to be reasonable to explain the experimental data. However, recent data from exclusive measurements with respect to angular momentum have not been properly explained by the available prescriptions of spin dependence of nuclear level density [2–4]. In these cases additional dependence on angular momentum was required, which was incorporated through the variation of the level density parameter with angular momentum. In one such measurement of angular-momentum-gated neutron evaporation spectra for $A \sim 118$, populated at excitation energies $E^* \sim 31$ and 43 MeV and angular momentum $J \sim 10\hbar$ to $20\hbar$, it has been observed that the inverse level density parameter decreases with increasing angular momentum, indicating a relative enhancement of NLD for higher J [3]. In another recent study, we have simultaneously measured all the (significant) light-particle evaporation spectra along with γ -ray multiplicity emitted from the compound nuclei $^{97}\text{Tc}^*$ and $^{62}\text{Zn}^*$ populated at $E^* \sim 36$ MeV and J in the range of $10\hbar$ to $20\hbar$. From the analysis of the all three (n , p , and α particle) light-particle spectra, a strong variation of the level density parameter with angular momentum was observed for both systems [2]. In this case also, the inverse level density parameter was found to decrease with increasing angular momentum. A strong variation of the inverse level density parameter with angular momentum was also reported in the measurement of angular-momentum-gated α -particle spectra for a number of nuclei with $A \sim 120$,

*pratap_presi@yahoo.co.in

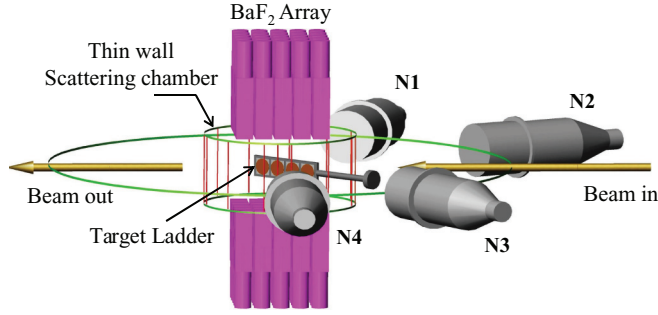


FIG. 1. (Color online) Schematic illustration of the experimental setup used in the present experiment.

$E^* \sim 60$ MeV, and $J \sim 10\hbar$ to $20\hbar$ in Ref. [4]. With the observed dependence of the level density parameter on J in the earlier studies it will be interesting to extend this study to different mass regions, specifically for heavier nuclei. With this aim we measured γ -ray-multiplicity-gated neutron evaporation spectra for the ${}^4\text{He} + {}^{197}\text{Au}$, ${}^4\text{He} + {}^{181}\text{Ta}$, and ${}^4\text{He} + {}^{165}\text{Ho}$ reactions at $E^* \sim 27$ and 37 MeV to extract the explicit angular-momentum dependence of NLD for heavier systems. The present results along with the earlier measurements in lighter systems are likely to help in understanding the systematics of the angular-momentum dependence of NLD at different mass regions in a better manner.

II. EXPERIMENTAL DETAILS

The present experiment was performed by using 28 and 40 MeV ${}^4\text{He}$ ion beams obtained from the K 130 cyclotron of the Variable Energy Cyclotron Centre in Kolkata, India. Self-supporting foils of ${}^{181}\text{Ta}$, ${}^{165}\text{Ho}$ (thicknesses ~ 1 mg/cm²) and ${}^{197}\text{Au}$ (thickness ~ 500 $\mu\text{g}/\text{cm}^2$) were used as targets to populate the compound nuclei ${}^{201}\text{Tl}^*$, ${}^{185}\text{Re}^*$, and ${}^{169}\text{Tm}^*$ from the ${}^4\text{He} + {}^{197}\text{Au}$, ${}^4\text{He} + {}^{181}\text{Ta}$ and ${}^4\text{He} + {}^{165}\text{Ho}$ reactions, respectively. To detect the neutrons emitted in the decay of the

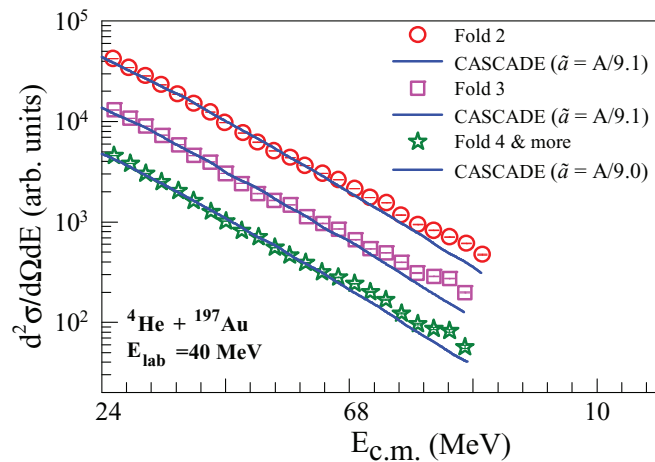


FIG. 2. (Color online) Experimental neutron energy spectra (symbols) for different folds along with the theoretical fits (continuous lines) made by using the statistical model code CASCADE for the ${}^4\text{He} + {}^{197}\text{Au}$ system at 40 MeV incident energy.

compound nuclei, four liquid-scintillator (BC501A) detectors of dimension 5 inch \times 5 inch were used [11]. The neutron detectors were placed outside the scattering chamber at angles 90° , 105° , 120° , and 150° with respect to the beam direction at a distance of 150 cm from the target. A schematic of the experimental setup used in the present measurement is shown in Fig. 1.

To keep the background of the neutron detectors at the minimum level, the beam dump was kept 3 m away from the target and was well shielded with layers of lead and borated paraffin. The energy of the emitted neutrons has been measured by using the time-of-flight (TOF) technique whereas the neutron gamma discrimination was achieved by both pulse-shape discrimination (PSD) and time of flight. In converting the neutron TOF to neutron energy, the prompt γ peak in the TOF spectrum was used as the time reference. The efficiency correction for the neutron detectors were performed by using the Monte Carlo code NEFF [12]. Neutrons emitted in these reactions were detected in coincidence with a 50-element BaF_2 -based low-energy γ -ray filter array [13], which was used to estimate the populated angular momenta of the compound nuclei and to provide the start signal for the TOF measurement. The filter was split into two blocks of 25 detectors each and were placed on the top and bottom of the thin-wall reaction chamber (wall thickness ~ 3 mm) in a staggered

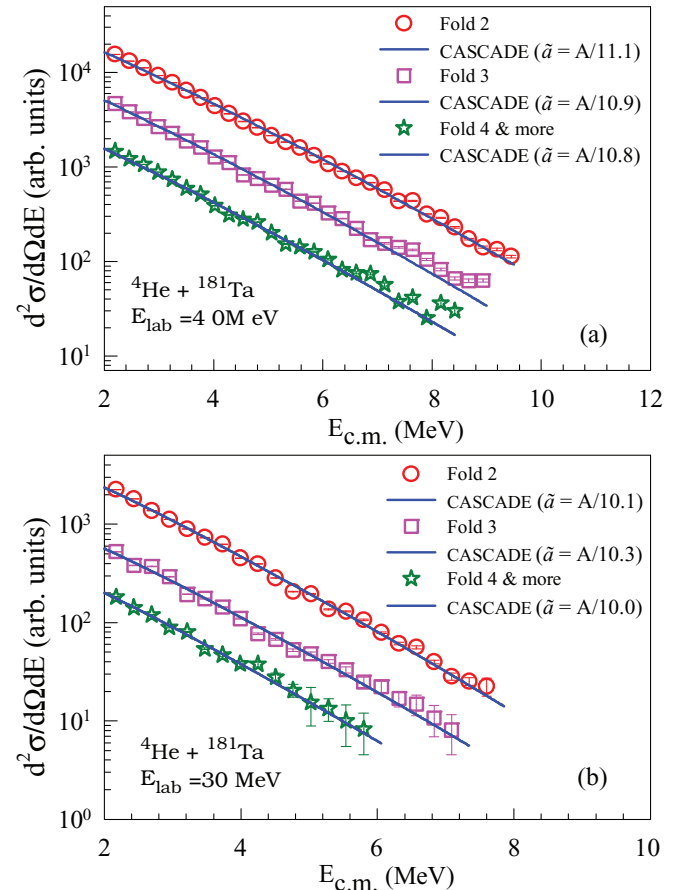


FIG. 3. (Color online) Same as Fig. 2 but for the ${}^4\text{He} + {}^{181}\text{Ta}$ system at (a) 40 MeV and (b) 30 MeV incident energies.

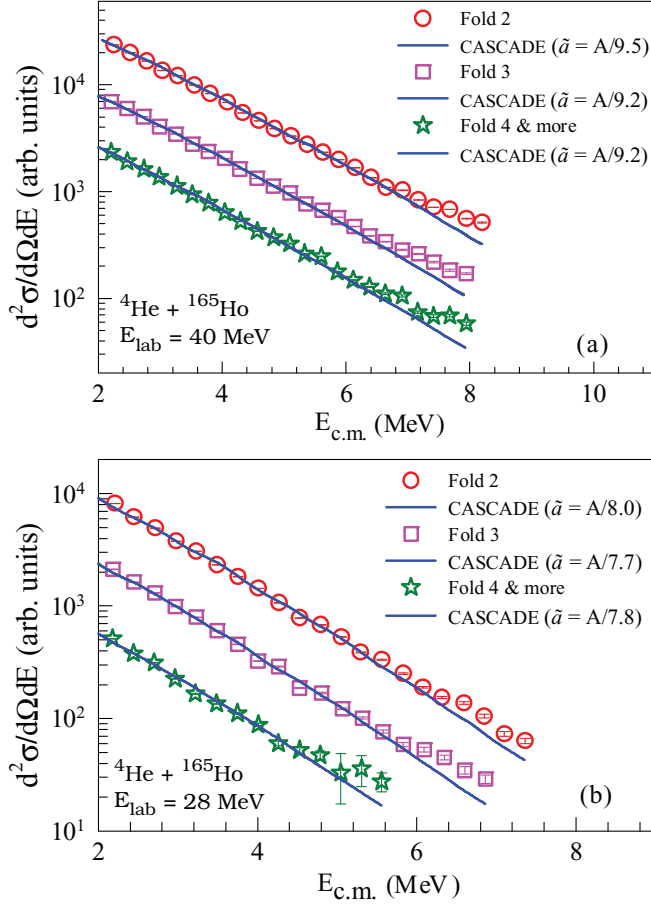


FIG. 4. (Color online) Same as Fig. 2 but for the ${}^4\text{He} + {}^{165}\text{Ho}$ system at (a) 40 MeV and (b) 28 MeV incident energies.

castle-type geometry (Fig. 1). Typical solid angle coverage of the multiplicity filter was about $\sim 33\%$. Data from the neutron detectors were recorded in event-by-event mode in coincidence with γ rays of different folds. Here “fold” is defined as the number of BaF_2 detectors fired simultaneously in an event, which is directly related to the populated angular momentum. The angular-momentum distributions for different folds were obtained by converting the measured γ -fold distribution using the Monte Carlo simulation technique based on the GEANT3 toolkit, by including real experimental conditions like detector threshold and trigger conditions in the simulation [13].

III. RESULTS AND DISCUSSIONS

The experimental neutron energy spectra for different γ folds were extracted and compared with the theoretical calculations performed with the statistical model code CASCADE [14] by using the extracted angular-momentum distributions for different folds as inputs. The fold-gated experimental neutron energy spectra for the ${}^4\text{He} + {}^{197}\text{Au}$, ${}^4\text{He} + {}^{181}\text{Ta}$, and ${}^4\text{He} + {}^{165}\text{Ho}$ systems, along with the corresponding CASCADE fits are shown in Figs. 2, 3, and 4, respectively. In the CASCADE calculation, the phenomenological level density formula predicted by the back shifted Fermi gas model [9]

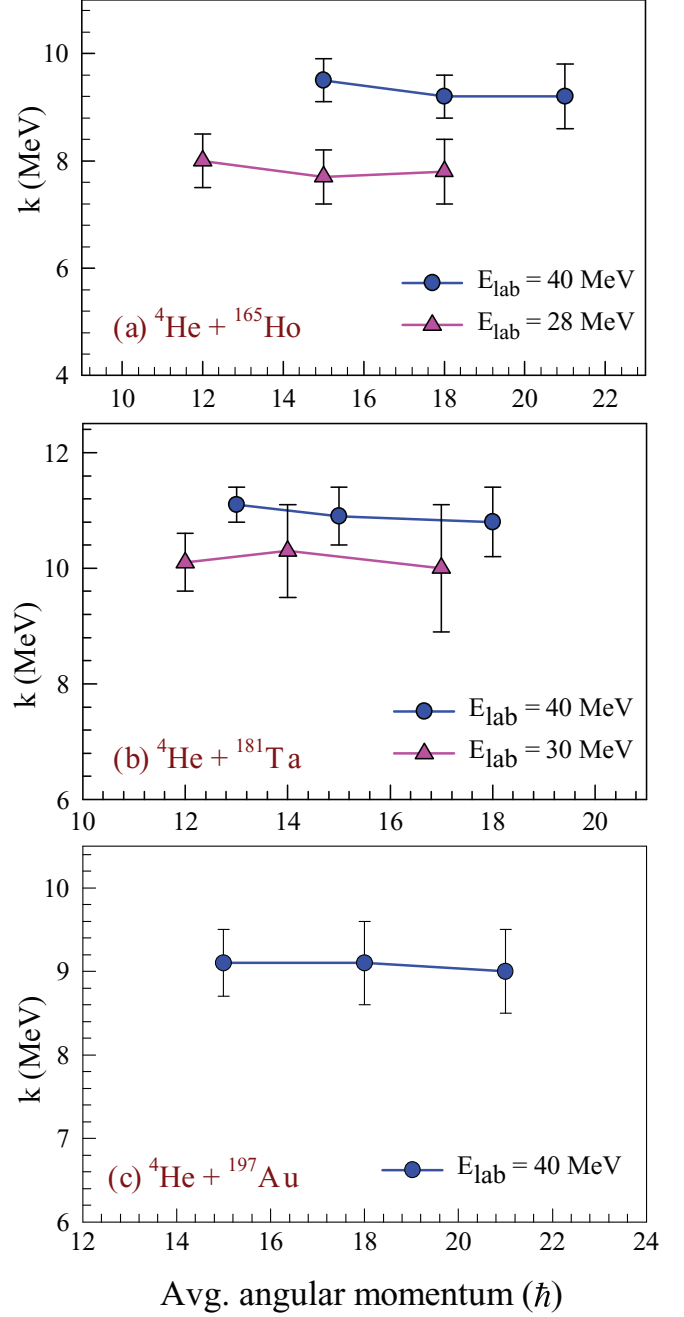


FIG. 5. (Color online) Variation of the inverse level density parameter with average angular momentum corresponding to different γ folds in the case of (a) ${}^4\text{He} + {}^{165}\text{Ho}$ (b) ${}^4\text{He} + {}^{181}\text{Ta}$, and (c) ${}^4\text{He} + {}^{197}\text{Au}$ systems.

given by

$$\rho_{\text{int}}(E^*, J) = \frac{(2J+1)}{12} \left(\frac{\hbar^2}{2\mathfrak{I}_{\text{eff}}} \right)^{3/2} \sqrt{a} \times \frac{\exp(2\sqrt{a(E^* - E_{\text{rot}} - \Delta\rho)})}{(E^* - E_{\text{rot}} - \Delta\rho)^2} \quad (3)$$

was used, where a is called the level density parameter, E^* is the excitation energy, and $\Delta\rho$ is the pairing energy. The NLD parameter a is related to the density of the single-particle

levels near the Fermi surface and is influenced by the shell structure and the shape of the nucleus, which in turn depend on the excitation energy. The shell effect and its dependence on excitation energy has been accounted for by the Ignatyuk formalism [15], which is expressed as

$$a = \tilde{a} \left[1 - \frac{\Delta S}{U} \{1 - \exp(-\gamma U)\} \right], \quad (4)$$

$$\gamma^{-1} = \frac{0.4A^{4/3}}{\tilde{a}}, \quad (5)$$

$$U = E^* - E_{\text{rot}} - \Delta_P, \quad (6)$$

where \tilde{a} is the asymptotic value of the liquid-drop NLD parameter at the excitation energy where shell effects are depleted. Here ΔS is the shell correction obtained from the difference of the experimental and the liquid-drop model masses and γ is the rate at which the shell effect is depleted with the increase in excitation energy. The quantity U is nothing but the available thermal excitation energy which contributes to the temperature. In the present formulation of $\rho_{\text{int}}(E^*, J)$ the spin dependence in NLD is incorporated through the spin-dependent rotational energy E_{rot} by using the rotating liquid drop model (RLDM) prescription as given by Eqs. (1) and (2). The shape of the neutron kinetic energy spectra in the statistical model calculation were mostly determined by the value of the level density parameter. The role of the deformability coefficients (δ_1 and δ_2) were found to be insignificant for the neutron spectra for all systems. The experimental spectra were fitted with the theoretical spectra

TABLE I. Average angular momenta and the extracted inverse level density parameters for different γ folds.

System	E_{lab} (MeV)	Fold	$\langle J \rangle$ (\hbar)	k (MeV)
${}^4\text{He} + {}^{197}\text{Au}$	40	2	15.0 ± 4.9	9.1 ± 0.4
${}^4\text{He} + {}^{197}\text{Au}$	40	3	18.0 ± 5.0	9.1 ± 0.5
${}^4\text{He} + {}^{197}\text{Au}$	40	≥ 4	21.0 ± 6.0	9.0 ± 0.5
${}^4\text{He} + {}^{181}\text{Ta}$	40	2	13.0 ± 4.0	11.1 ± 0.3
${}^4\text{He} + {}^{181}\text{Ta}$	40	3	15.0 ± 4.0	10.9 ± 0.5
${}^4\text{He} + {}^{181}\text{Ta}$	40	≥ 4	18.0 ± 5.0	10.8 ± 0.6
${}^4\text{He} + {}^{181}\text{Ta}$	30	2	12.0 ± 4.0	10.1 ± 0.5
${}^4\text{He} + {}^{181}\text{Ta}$	30	3	14.0 ± 4.0	10.3 ± 0.8
${}^4\text{He} + {}^{181}\text{Ta}$	30	≥ 4	17.0 ± 5.0	10.0 ± 1.1
${}^4\text{He} + {}^{165}\text{Ho}$	40	2	15.0 ± 4.9	9.5 ± 0.4
${}^4\text{He} + {}^{165}\text{Ho}$	40	3	18.0 ± 5.0	9.2 ± 0.4
${}^4\text{He} + {}^{165}\text{Ho}$	40	≥ 4	21.0 ± 6.0	9.2 ± 0.6
${}^4\text{He} + {}^{165}\text{Ho}$	28	2	12.0 ± 4.0	8.0 ± 0.5
${}^4\text{He} + {}^{165}\text{Ho}$	28	3	15.0 ± 5.0	7.7 ± 0.6
${}^4\text{He} + {}^{165}\text{Ho}$	28	≥ 4	18.0 ± 6.0	7.8 ± 0.6

by varying the level density parameter, which is estimated as $\tilde{a} = A/k$, where k is called the inverse level density parameter. The optimum values of k were extracted by fitting the experimental neutron spectra using the χ^2 minimization technique. The extracted values of the inverse level density parameter as obtained for different average angular momenta corresponding to different γ folds are shown in Table I. The variation of k with $\langle J \rangle$ for the present systems has been plotted in Fig. 5. It can be observed from the figure that the values

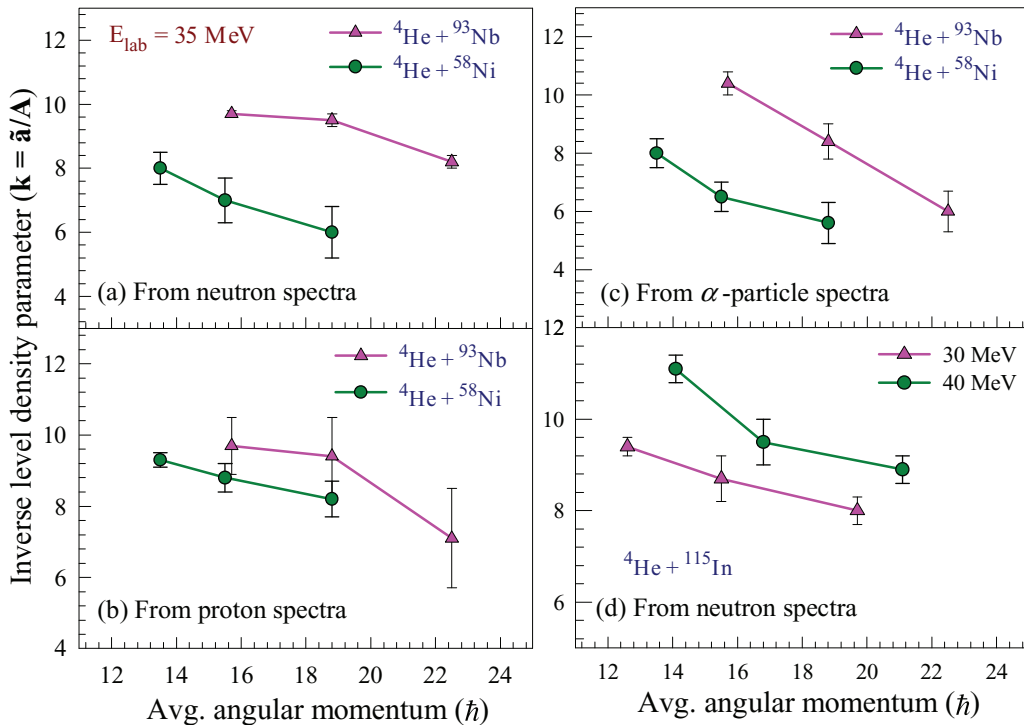


FIG. 6. (Color online) Variation of the inverse level density parameter with average angular momentum for the ${}^4\text{He} + {}^{93}\text{Nb}$ (filled triangle) and ${}^4\text{He} + {}^{58}\text{Ni}$ (filled circle) systems as observed from the analysis of the (a) neutron, (b) proton, and (c) α -particle spectra and (d) for the ${}^4\text{He} + {}^{115}\text{In}$ system as observed from the analysis of the neutron evaporation spectra at $E_{\text{lab}} = 30$ MeV (filled triangles) and $E_{\text{lab}} = 40$ MeV (filled circles). Data were taken from Refs. [2,3], respectively.

of the inverse level density parameter remains almost constant for all the folds (angular momentum) in all three cases. For the sake of comparison, the extracted k values at different folds in the case of lighter nuclei populated around similar excitation energy and angular-momentum range through the ^4He -induced reactions are shown in Fig. 6. It is seen from the figure that, for the light- and medium-mass nuclei (^{62}Zn , ^{97}Tc , and ^{119}Sb) there is a substantial decrease in the k value at higher angular momentum. On the contrary, the k value remains almost constant at all the folds in case of the relatively heavier systems (Fig. 5). It is therefore interesting to note that, for light- and medium-mass nuclei (^{119}Sb , ^{62}Zn , and ^{97}Tc) measured neutron (as well as charged particles) evaporation spectra in coincidence with γ -ray multiplicity gave a clear signature of the angular-momentum dependence of the level density parameter, while for heavier nuclei (^{201}Tl , ^{185}Re , and ^{169}Tm) no such dependence on angular momentum was observed. It may be noted that the value of the spin cutoff parameter (σ) for the current systems are in the range of $10.5\hbar$ to $15.5\hbar$, which is of similar magnitude to that of the populated angular momenta. The nearly constant nature of the level density parameter with the variation in angular momentum in the 180 mass region has also been reported by Gupta *et al.* [5] from the measurement of the fold-gated α -particle evaporation spectra. However, a strong dependence of k on J was observed from similar measurements in the $A \sim 120$ mass region by the same group [4], as already described in the introduction. The present result as well as the earlier measurements as discussed above indicates that

angular-momentum dependence of NLD may have sensitivity to the mass number. However, to comprehensively understand the angular-momentum dependence of NLD and its sensitivity over the mass region, more exclusive measurements at different mass regions are required.

IV. SUMMARY AND CONCLUSION

The energy spectra of the neutrons emitted in the decay of $^{201}\text{Tl}^*$, $^{185}\text{Re}^*$, and $^{169}\text{Tm}^*$ have been measured at backward angles in coincidence with the γ rays of different multiplicities. The analysis of γ -ray-fold-gated neutron spectra has been carried out by using the statistical model code CASCADE. From the present data it is observed that the k value remains almost constant with the change in angular momentum. The present observation is in contrast to the earlier observed trend from similar measurements for the light- and medium-mass nuclei. The different trends of variation of k with J as observed in different mass regions indicate that the angular-momentum dependence of NLD as described by the spin dependent rotational energy along with the shape change at higher angular momentum using the RLDM prescription is sufficient to explain the experimental data at the $A \sim 180$ mass region, which was found to be inadequate in earlier measurements at the lower-mass regions.

ACKNOWLEDGMENT

The authors are thankful to the VECC Cyclotron operators for smooth running of the accelerator during the experiment.

-
- [1] M. Gohil *et al.*, *EPJ Web Conf.* **66**, 03073 (2014).
 [2] Pratap Roy *et al.*, *Phys. Rev. C* **86**, 044622 (2012).
 [3] K. Banerjee *et al.*, *Phys. Rev. C* **85**, 064310 (2012).
 [4] Y. K. Gupta, Bency John, D. C. Biswas, B. K. Nayak, A. Saxena, and R. K. Choudhury, *Phys. Rev. C* **78**, 054609 (2008).
 [5] Y. K. Gupta, D. C. Biswas, Bency John, B. K. Nayak, A. Saxena, and R. K. Choudhury, *Phys. Rev. C* **80**, 054611 (2009).
 [6] A. Mitra, D. R. Chakrabarty, V. M. Datar, Suresh Kumar, E. T. Mirgule, and H. H. Oza, *Nucl. Phys. A* **707**, 343 (2002).
 [7] A. Bohr and B. R. Mottelson, *Nuclear Structure* (Benjamin, New York, 1975), Vol. 1.
 [8] S. Cohen, F. Plasil, and W. J. Swiatecki, *Ann. Phys. (NY)* **82**, 557 (1974).
 [9] H. A. Bethe, *Phys. Rev.* **50**, 332 (1936); *Rev. Mod. Phys.* **9**, 69 (1937).
 [10] R. G. Stokstad, in *Treatise on Heavy Ion Science*, edited by D. Bromley (Plenum, New York, 1985), Vol. 3, p. 83.
 [11] K. Banerjee *et al.*, *Nucl. Instrum. Methods Phys. Res., Sect. A* **608**, 440 (2009).
 [12] G. Dietze and H. Klein, PTB-ND-22 Report, 1982.
 [13] Deepak Pandit, S. Mukhopadhyay, Srijit Bhattacharya, Surajit Pal, A. De, and S. R. Banerjee, *Nucl. Instrum. Methods Phys. Res., Sect. A* **624**, 148 (2010).
 [14] F. Puhlhofer, *Nucl. Phys. A* **280**, 267 (1977).
 [15] A. V. Ignatyuk, G. N. Smirenkin, and A. S. Tishin, *Sov. J. Nucl. Phys.* **21**, 255 (1975).